Materials Science in Semiconductor Processing 86 (2018) 79–84

Contents lists available at ScienceDirect

Materials Science in Semiconductor Processing

journal homepage: www.elsevier.com/locate/mssp

Synthesis of WO_3 nanorods by thermal oxidation technique for NO_2 gas sensing application

Bhagaban Behera[a,*], Sudhir Chandra[b]

[a] Centre for Applied Research in Electronics, Indian Institute of Technology Delhi, Hauz Khas, New Delhi 110016, India
[b] Electronics and Communication Department, Bennett University, Plot No. 8-11, Tech Zone-II, Greater Noida 201310, UP, India

ARTICLE INFO

Keywords:
WO_3 Nanorods
NO_2
Gas sensor
Selective detection

ABSTRACTS

In this work, WO_3 nanorods were successfully synthesized by thermal oxidation method and further investigated for gas sensing application. For WO_3 nanorods synthesis, tungsten film was deposited on oxidized Si substrate by sputtering method and subsequently subjected to thermal oxidation process at 500 °C in atmospheric environment. The synthesized nanorods were analyzed using SEM, XRD, Raman, and XPS. A chemiresistive type MEMS-based sensing device was fabricated incorporating these nanorods. The sensor was tested for different gases and VOCs over operating temperatures ranging from 75 to 300°C. It showed high selectivity towards NO_2 gas over H_2S, NH_3, acetone, methanol, and ethanol. The excellent sensing performance and sophisticated method of synthesis make this a promising candidate for gas sensing applications.

1. Introduction

High-performance gas sensors have gained increasing attention due to their diverse applications such as pollutant detection, medical diagnosis, chemical monitoring, food processing etc. Day by day, the amount of air pollutants such as NH_3, CO, SO_2, H_2S NO_2, and volatile organic compounds (VOCs) exhaust from combustible engines, automobiles are increasing [1]. NO_2 is one of the major pollutants found in the atmosphere which causes acid rain, ozone layer thinning and respiratory related diseases. Thus, an efficient NO_2 sensor needs to be developed for environmental monitoring and protection of humans from over-exposure.

Over the last decade, research has been devoted considerable efforts for development of sensitive and reliable gas sensor. Various semiconducting metal oxides such as SnO_2, ZnO, CuO, WO_3, In_2O_3, and TiO_2 have been used as sensing material [2–7]. Among these, tungsten oxide (WO_x) has received considerable attention as a promising sensing material due to its high sensitivity and stability, specifically towards NO_2 gas [5,8–11]. Various WO_3 nanostructures such as nanoparticles, nanowhisker, nanorods, and nanowires have shown enhanced sensing properties towards different gases [12–15]. The prime reason for such enhancement is due to improvement in surface area to volume ratio which propels the chemical interaction between analytes and sensing element. Till date, several methods such as thermal evaporation, chemical vapor deposition, electro-spinning, sol-gel, chemical bath deposition, hydrothermal and template-directed synthesis have been used for synthesis of these WO_3 nanostructures [10–13,16–22]. All these methods have certain limitations such as (i) high thermal budget (ii) complicated processing technique (iii) use of catalyst (iv) long processing time (v) high cost (vi) adaptability for mass production, (vii) unwanted byproducts (vii) not being environment-friendly. Among these methods, sol-gel and chemical bath depositions are economical, low temperature, and mass production worthy process. However, the sol-gel films create uncontrolled porosity, weak adhesion to substrate and unwanted cracks. On the other hand, chemical bath deposition and hydrothermal methods produce unwanted byproducts after each deposition.

In the field of sensor technology, intensive research is in progress for optimal sensing performances by controlling grain sizes, shapes, porosities and/or active surface areas and makes it compatible with post-CMOS processing [23]. Nanostructures synthesis by thermal oxidation technique is simple, cost-effective, and production worthy method. Nanostructures of ZnO, CuO and F_2O_3 have been successfully synthesized by thermal oxidation technique [3,24,25]. There are only few reports on synthesis of tungsten nanostructures by thermal oxidation technique and thus more studies are needed on this method for different applications [5,26].

In this work, WO_3 nanorods are synthesized by thermal oxidation technique in atmospheric environment from sputter deposited tungsten film. Post-oxidized sample was analyzed using various techniques such as scanning electron microscopy (SEM), X-ray diffraction (XRD), Raman Spectroscopy and X-ray photoelectron spectroscopy (XPS) to study its

* Corresponding author.
E-mail address: bhagaban7044@gmail.com (B. Behera).

https://doi.org/10.1016/j.mssp.2018.06.022
Received 16 May 2018; Received in revised form 14 June 2018; Accepted 23 June 2018
1369-8001/

morphology, crystalline nature, and chemical composition. A microelectromechanical systems (MEMS) based sensing device was fabricated incorporating nanorods and their performances towards different VOCs (ethanol, acetone, and methanol) and toxic gases (NH_3, H_2S and NO_2) were evaluated. The sensor's response over different operating temperature and concentrations was evaluated for optimal sensing performances.

2. Experimental works

Tungsten metal film of thickness 100 nm was deposited on SiO_2 coated Si substrate using RF sputtering technique. The deposited film was oxidized in a horizontal tube furnace at 500 °C for 4 h in atmospheric ambient. Post-oxidized sample's morphology was observed using SEM (Model: Zeiss, EVO 18) and its crystallography was analyzed using XRD (Model: Phillips X'pert, Cu Kα X-ray source with a wavelength of 1.54 Å) and Raman Spectroscopy (Model: HORIBA, LabRAM HR Evolution, laser source: 514 nm). The chemical composition of nanorods was studied using XPS (Model: SPECS, Phoibos 100). After WO_3 nanorods growth, a sensor was fabricated using planar MEMS technology as mentioned in our previous publication [4]. The device consists of a micro-heater and surrounding IDE (Inter Digited Electrode) structure and both of these are placed on solid thermal insulator. A schematic diagram of micromachined gas sensor and its optical image are shown in Fig. 1. The size of the device was 1.21 mm^2 and had minimum feature size 40 µm. This device was fabricated by following various microfabrication steps such as oxidation, photolithography, anisotropic etching, deposition, chemical mechanical polishing and lift-off. In this micromachined platform, a solid thermal insulator (6 µm thick of SiO_2) was created by burying it into the silicon substrate. This platform reduces heat spreading from localized area and thus power consumption is reduced [4]. The temperature is generated by a joule heating when a voltage is applied across the terminals of the micro-heater. For calibration purpose, a dc voltage was applied through source pads and simultaneously, the current was measured between the two pads i.e. resistance was measured at different voltage. In a separate experiment, microheater resistance was measured at different temperatures by keeping it on a stabilized hot plate. Resistance measured by both these techniques were compared and calibrated to find out temperature of the heater when a voltage was applied during actual operation of the sensor [27–29]. Thus, the temperature of the micro-heater was not measured directly but estimated by characterizing the current-voltage and resistance-temperature curves of the microheater. The nanorods resistance was measured using a resistance meter (Keithely 2400) connected across IDE structure. The sensor was tested for different VOCs (ethanol, acetone, and methanol) and toxic gases (NH_3, H_2S and NO_2) of concentration 2–50 ppm at different operating temperature. The sensor sensitivity also known as response magnitude is defined as [30]:

$$S = \frac{R_a - R_g}{R_g} \times 100\% \quad \text{(for reducing gas)}$$
$$S = \frac{R_g - R_a}{R_a} \times 100\% \quad \text{(for oxidizing gas)} \tag{1}$$

Where R_g and R_a are the resistance of nanorods in presence and absence of target gas respectively. The sensing was evaluated to find out parameters for optimal sensing performance.

3. Results and discussion

Fig. 2(a) shows SEM image of as-deposited 100 nm thick tungsten film. Subsequently, the sample is oxidized at 500 °C for 4 h in atmospheric environment and its SEM is presented in Fig. 2(b). It is observed that uniformly distributed nanorods having diameter ~ 80 nm and length and ~ 400 nm are formed.

Post-oxidized sample's XRD pattern is shown in Fig. 3(a). The pattern is indexed as (002), (020), (211), (022), (222), 132) and (004) of monoclinic-WO_3. Also, it confirms that the nanorods are polycrystalline with monoclinic phase having lattice parameters a = 7.300 Å, b = 7.538 Å, c = 7.689 Å and β = 90.892° (JCPDS 75–0192). The intensity of (002) diffraction peak is strongest indicating most of the nanorods fabric axis is along the [002] direction. The grain size of nanorod was calculated using Scherrer's formula

$$D = \frac{k\lambda}{\beta cos\theta}$$

Where k represents Scherrer's constant, λ is 1.54 Å and β is FWHM of XRD peak. The nanorods average grain size is 26 nm.

Fig. 3(b) shows Raman spectra of synthesized nanorods. It can be observed that peaks are sharp indicating nanorods are crystalline in nature. In general tungsten oxides show two characteristics peaks corresponding to stretching range (200–400 cm^{-1}) and bending range (600–900 cm^{-1}). The recorded spectrums are compared with previously published results, which indicate that nanorods are in monoclinic phase [31]. The peak at 273.3 and 326.6 cm^{-1} represents bending vibration of W–O–W. The peaks 690.4 and 807.1 cm^{-1} represents asymmetric and symmetric vibration of W^{6+}–O bonds in stretching mode [31,32].

Chemical states of nanorods were studied using XPS technique. Fig. 4 shows XPS core level spectra of W 4f and O 1s. All these peaks

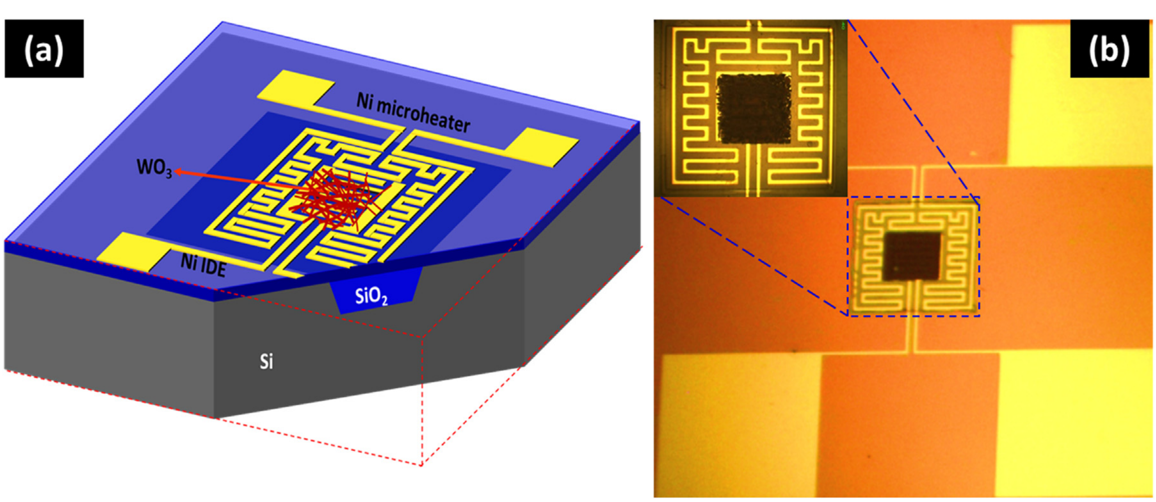

Fig. 1. (a) Schematic diagram of micromachined gas sensor (b) Optical image of the sensing device.